

FuncPipe: A Pipelined Serverless Framework for Fast and Cost-efficient Training of Deep Learning Models

Yunzhuo Liu
Shanghai Jiao Tong University

Bo Jiang
Shanghai Jiao Tong University

Tian Guo
Worcester Polytechnic Institute

Zimeng Huang
Shanghai Jiao Tong University

Wenhao Ma
Shanghai Jiao Tong University

Xinbing Wang
Shanghai Jiao Tong University

Chenghu Zhou
Chinese Academy of Sciences

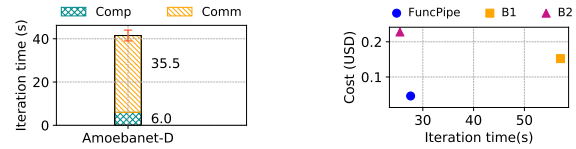
Abstract

Training deep learning (DL) models has become a norm. With the emergence of serverless computing and its benefits of true pay-as-you-go pricing and scalability, systems researchers have recently started to provide support for serverless-based training. However, the ability to train deep learning models on serverless platforms is hindered by the inherent limitations of today’s serverless infrastructure and the explosive requirement on memory and bandwidth. For example, existing AWS serverless functions have up to 10GB memory and 70MB/s bandwidth while training an AmoebaNet-D model with batch size 64 can require 45GB memory and transfer 900MB data per iteration. The appalling resource mismatch between serverless functions and DL models has stalled the progress on serverless-based training.

In this paper, we present FUNCPIPE, the first pipelined serverless framework that enables fast and low-cost training of DL models. FUNCPIPE is designed with the key insight that model partitioning can be leveraged to bridge both memory and bandwidth gaps between the capacity of serverless functions and the requirement of DL training. Conceptually simple, we have to answer a number of design questions including how to partition the model, how to configure each serverless function, and how to exploit each function’s uplink/downlink bandwidth. We co-optimize model partition and resource allocation with a Mixed-Integer Quadratic Programming formulation and redesign storage-based communication for efficient bandwidth usage. We implement FUNCPIPE on AWS and AliCloud and show that it achieves up to 77% cost savings and 2.2X speedup comparing to state-of-the-art serverless-based frameworks.

1 Introduction

Serverless computing has recently been exploited for distributed training as an alternative to traditional VM-based training [9, 27, 56, 60]. Serverless-based training has many attractive properties: it relieves machine learning practitioners from resource management tasks [9, 56]; it exhibits good



(a) LambdaML performance. (b) Training with three configurations.

Figure 1: **(a)** LambdaML encounters communication bottleneck when training an AmoebaNet-D model. **(b)** There is large room for training cost and time improvement with optimized model partition and serverless resource configuration.

resource elasticity and can auto-scale to many serverless workers for increased parallelism [53, 56]. However, today’s serverless infrastructures exhibit inherent limitations on available memory and bandwidth that make it difficult to directly utilize them to train resource-intensive DL models. As such, recent serverless-based training frameworks mostly focus on systems techniques to enable model training [27, 60], but still fall short in supporting fast and cost-efficient training due to the following reasons:

- Serverless functions have *very limited communication capability* that does not meet the growing communication demand for training DL models. The network bandwidth of a serverless function is typically very small. For instance, the maximum bandwidth of an AWS Lambda function is only about 70 MB/s [28, 57]. Moreover, serverless functions lack the ability of direct inter-function communication, which makes recent serverless-based training frameworks resort to two-hop communication via intermediary cloud storage such as Amazon S3 [27, 56]. Compounding with other design options such as data parallelism, existing serverless-based training frameworks can suffer severe communication bottleneck. Fig. 1(a) shows the iteration time for training a 900MB *AmoebaNet-D* with 8 AWS Lambda functions using LambdaML [27], a state-of-the-art serverless-based training framework. Note that computation takes only 6s

while communication takes nearly 36s.

- Serverless functions are allowed much smaller memory footprint than traditional VMs, hindering their ability to achieve cost-efficient computation-to-communication ratio. The memory consumption during training increases with the model size and the activation size, the latter being proportional to the batch size. Today’s serverless platform, e.g. AWS Lambda, offers up to 10GB memory size for a serverless function [5], which often falls short for training with a large batch size. For example, increasing the computation-to-communication ratio of the *AmoebaNet-D* from 0.17 in Fig. 1(a) to 0.5 (with local batch size ≈ 32) would require about 30GB memory, far above the current memory cap of AWS Lambda. Existing serverless-based training frameworks provide no solution for this low computation-to-communication ratio [9, 27, 56].

Our work aims at improving the speed and cost-efficiency of training DL models on serverless platforms. We address the above challenges through two major approaches, *utilizing model partition techniques* and *improving storage-based communication efficiency*. Our key insight is that model partitioning is not only good for overcoming the memory limitation, but also useful in relieving the communication burden in training. More specifically, to reduce the long communication time caused by the small bandwidth, we utilize model partition to reduce the amount of gradients of each serverless worker. Although greatly reduced through partition, the communication may still take up a large proportion of training time. We identify that the recently proposed storage-based scatter-reduce communication scheme [27] fails to simultaneously utilize the uplink/downlink bandwidth of serverless functions. To further speedup the communication, we redesign the scatter-reduce scheme that pipelines the upload and download to improve network utilization. Also, we are able to increase the computation to communication ratio as partitioned model allows a larger training batch size on each serverless function.

At the core, our work explores pipeline parallelism [14, 21, 38, 48], a type of parallel structure based on model partition, for *fast and low-cost* serverless-based training. We answer two key design questions: (i) how to partition the DL model; and (ii) how to allocate resource for each serverless function. These two questions pose a more complicated optimization question, compared to existing server-based pipelined training [14, 38, 51]. Specifically, those prior work often assume static training resources, i.e., a fixed number of workers with fixed resources, and with the goal to only maximize training throughput. In contrast, our work tackles both model partition and resource allocation to workers to optimize for both training throughput and cost. Fig. 1(b) compares the performance of training an *AmoebaNet-D* with the model partition and serverless resource allocation configurations found by FUNCPIPE and two existing algorithms (denoted by B1 and B2). We can see a large space for improvement: training

with configuration found by FUNCPIPE reduces 52%/70% iteration time/cost compared to B1, and reduces cost by 80% compared to B2 with only 8% time overhead.

In short, we make the following main contributions.

- We design and implement FUNCPIPE, the first pipelined serverless framework that enables fast and cost-efficient training of DL models. FUNCPIPE provides user-friendly Python APIs that require minimal changes to user code.
- We propose a novel pipelined scatter-reduce scheme that better utilizes the uplink/downlink bandwidth during model synchronization. Our scheme reduces the synchronization time by up to 26% and the overall iteration time by up to 18% compared to the non-pipelined scatter-reduce in [27].
- We formulate a co-optimization problem for model partition and resource allocation using Mixed-Integer Quadratic Programming (MIQP). Our approach finds configurations that achieve up to 80% higher training speed and 55% lower cost compared to existing approaches [8, 51].
- We conduct extensive evaluation of FUNCPIPE on two public serverless platforms with representative DL models. FUNCPIPE improves the training speed by up to 2.2X while reducing the training cost by 77%, compared to LambdaML, the state-of-the-art serverless training framework [27].

2 Background

2.1 Serverless Computing

Serverless computing provides a new paradigm for deploying applications. To use serverless computing on major platforms such as AWS Lambda [5], users upload their applications as stateless serverless functions and need to configure the functions with the proper amount of resources. Serverless users can execute the functions and obtain the computation results without having to manage the underlying computation resources such as VMs. The task of resource configuration in today’s serverless platforms amounts to deciding the memory allocation; given a memory allocation, other resources like CPU and network bandwidth are allocated proportionally. Further, users are charged proportional to the allocated memory and the actual runtime of their program.

Serverless computing makes it easy to trigger many instances of the same serverless function (up to thousands) concurrently; each function instance is often ready to run within seconds or even milliseconds depending on the cold-start [35, 54]. Serverless provides the true *pay-as-you-go* pricing models and has garnered high interests from both industry and academia [1, 13, 20, 42] to run event-driven workloads such as in-memory caching [44, 45, 55] and workloads that benefit from high degree of parallelism including distributed

training [9,27,56,60]. In this work, we are interested in extending serverless computing’s benefits toward fast and low-cost distributed training of deep learning models.

2.2 Distributed Training

Distributed training refers to the process of training a machine learning model with multiple workers that communicate over NVLink or over network [11,64]. The essence of distributed training boils down to determine how to divide tasks among workers and how to communicate progress.

Parallelism. The most widely adopted type of parallelism is *data parallelism* [30,46], where each worker maintains a replica of the entire model and a split of the dataset. In a training iteration, i.e. the processing of one batch of data, workers calculate the gradients on their local data and then exchange the gradients with each other and update the model parameters. Another type is *model parallelism* [7,10,22] where the model is partitioned across workers. Rather than compute the gradients for the entire model, each worker will only compute the data batch on the assigned partition and then communicate the output to the next worker. Consequently, model parallelism often leads to reduced memory consumption and communication data size on each worker. Data parallelism can be further combined with model parallelism by having multiple replicas for each model partition [6,17,25]. In such case, workers working on the same partition need to synchronize gradients with each other. Compared with data parallelism, hybrid parallelism reduces worker-to-worker communication as only gradients for partitions are exchanged. Our work leverages pipeline parallelism where we partition the model and allows data parallelism for each partition, as further describe in § 2.3. It falls under the general hybrid parallelism.

Synchronization. Today’s distributed training frameworks either resort to centralized or decentralized synchronization architectures. Parameter Server (PS)-based architecture is a typical centralized structure where workers upload their gradients to a central server and from whom fetch the latest updated model [32,33]. A recently proposed serverless-based training framework Cirrus [9] uses a VM as a parameter server and serverless instances as workers. We refer to a mix of traditional VMs and serverless workers as *hybrid PS* structure. In decentralized synchronization, workers communicate with each other following the steps of the specific communication algorithms, such as all-reduce [40,41,43,52] and scatter-reduce [52]. LambdaML [27] proposes the most recent storage-based scatter-reduce method. Finally, distributed training can either use synchronous or asynchronous protocols to instruct when workers can proceed to work on the next data batch. Synchronous protocol, in essence, allows workers to work on the same version of model parameters and therefore is not subject to potential accuracy convergence issues faced by asynchronous training [34,63]. In this work, we use de-

centralized synchronous training with the goal to fully exploit worker bandwidth and avoid impact on converged accuracy.

2.3 Pipeline Training

Pipeline parallelism has been explored as a technique to improve the resource utilization of traditional server-based distributed training [14,21,31,38,48]. At a high level, pipeline parallelism divides a data batch into micro-batches and treats each model partition as a stage in the pipeline. During the training, micro-batches will be scheduled to go through the model partitions in a pipelined fashion to simultaneously utilized resources of different stages. As such, pipeline parallelism can address the low resource utilization problem of model parallelism by reducing the worker idle time.

One of the key challenges in applying pipeline parallelism to distributed training is to ensure training efficiency. For example, unoptimized model partition can lead to imbalanced stage time or cause long inter-stage communication time, hindering the overall training performance. The problem of configuring pipeline parallelism often comes down to partitioning the model and assigning partitions to workers. Prior work on server-based training has proposed various model partition strategies to improve training throughput [14,38,51]; however, they often assume static training resources, i.e., a fixed number of workers with fixed resources. In serverless computing, we are presented with the flexibility to scale up to many workers and to easily configure workers with different amount of resources. Such flexibility is a double-edged sword: it gives us more knobs to improve the performance and reduce the monetary cost, while it also makes the problem of configuring pipeline parallelism more difficult. In this work, we tackle the challenge of effectively configuring pipeline parallelism in a serverless-based training environment to achieve high throughput and incur low cloud bills.

3 FUNCPIPE

In this section, we present FUNCPIPE, a novel pipelined serverless framework for efficient training of DL models. § 3.1 provides an overview of the system architecture and workflow. § 3.2 and § 3.3 give detailed designs of the main training pipeline and pipelined scatter-reduce, respectively. § 3.4 presents our co-optimization approach for model partition and resource allocation.

3.1 System Overview

System Architecture. As shown in Fig. 2, FUNCPIPE consists of three parts, startup components, runtime components and client-side APIs. The startup and runtime components are displayed in the two gray boxes in the figure, represented by blue and yellow boxes respectively. Those components

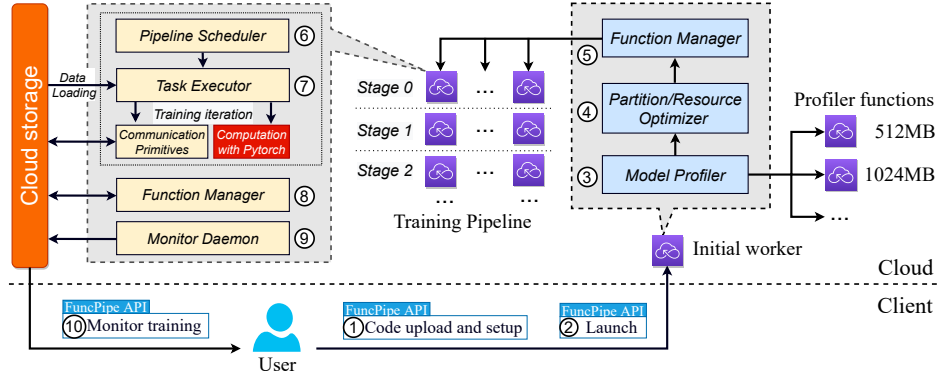


Figure 2: **FUNCPIPE system architecture and workflow.** The two gray boxes enclose FUNCPIPE components. The blue blocks are the startup components active in the initial worker, and the yellow blocks are the runtime components in a training worker.

run on the serverless platform and interact with cloud storage and client-side APIs. The client-side APIs enable the users to setup, launch, and monitor the training with minimum effort.

Workflow. The workflow of FUNCPIPE is shown in Fig. 2. The user first prepares the training code using FUNCPIPE APIs, and then sets up and launches training from the client side (① and ②). At the beginning, an initial worker with the startup components performs the preparation work: ③ *Model Profiler* profiles model layers on serverless functions with different memory allocations; ④ With the gathered layer-wise information, e.g., computation time, parameter and activation size, *Partition/Resource Optimizer* finds the optimal model partition and the best resource allocation basing on our MIQP formulation (§ 3.4); ⑤ *Function Manager* launches and configures all training workers to start the pipeline.

When the pipeline training starts, micro-batches are scheduled to traverse the pipeline: ⑥ *Pipeline Scheduler* in each worker decides their order in processing the micro-batches. ⑦ *Task Executor* handles the processing tasks by interacting with the underlying storage-based *Communication Primitives* and *Pytorch*. It properly overlaps the communication and computation. ⑧ *Function Manager* on each worker exchanges information during training to ensure the health of the pipeline; it checkpoints and restarts the worker at designated time interval to deal with serverless function timeout. ⑨ *Monitor Daemon* gathers and uploads training information that the user can access using client-side API (⑩).

3.2 Main Training Pipeline

We illustrate the pipeline design of FUNCPIPE through the example in Fig. 3. The pipeline performs synchronous training that avoids potential accuracy convergence issues. FUNCPIPE partitions the model and places each partition on a serverless worker. In a training iteration, the data batch is divided as micro-batches (the ID of each micro-batch is labeled on its corresponding blocks in Fig. 3) and they are scheduled to traverse the partitions in the following order: (i) all micro-batches go

through each partition to perform forward computation; (ii) after all forward computation have finished, the micro-batches go in a reversed order for backward computation, i.e. back-propagation. Our micro-batch scheduling policy is similar to the one in GPipe [21], a pipeline design for server and GPU based training. Each worker in our pipeline generally handles two types of tasks, computation and communication. Communication tasks are further divided into *upload*, *download*, and *sync*. The output of the partitions are communicated through *upload* and *download* to/from the cloud storage; *sync* is required at the end of a training iteration if multiple workers are configured for a partition (i.e., data parallelism). It can be performed as soon as the backward computation of the partition is completed.

Communication Optimization. A key difference between serverless and server-based pipelines is the proportion of communication time in the overall training time. In the server-based case, communication time is usually negligible as its workers can have large bandwidth, e.g., 100Gb RDMA or 300Gb NVlink. In the serverless case, however, it can take up a large proportion as serverless functions have limited bandwidth. Both *upload* and *download* times can be comparable to *computation* time, and *sync* time can even be significantly longer depending on the degree of data parallelism. For *upload* and *download*, our solution is to treat them as independent pipeline stages and overlap them with each other and the *computation* tasks. For *sync*, we design a pipelined scatter-reduce scheme in § 3.3.

Discussion on Micro-batch Scheduling. There exist other micro-batch scheduling policies [14, 23, 31]. These policies, designed for server-based training, aim to reduce memory consumption. In the serverless case, however, a smaller memory allocation is not necessarily desirable. As other resources like CPU and bandwidth are allocated proportionally to memory, it can slow down computation and communication and hence incur a higher cost due to increased training time. Moreover, more complicated scheduling also complicates the model par-

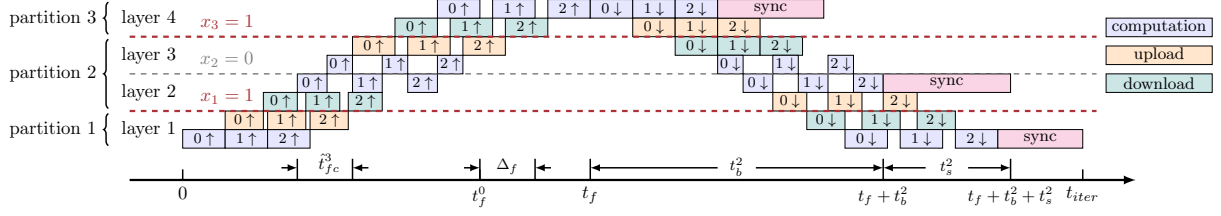


Figure 3: Main training pipeline of FUNCPIPE.

tition and resource allocation problem in §3.4. We leave it for future work to explore different scheduling.

3.3 Pipelined Scatter-reduce

We identify one of the reasons for the low communication efficiency in existing serverless-based training frameworks [27] as that the current storage-based synchronization design fails to make efficient use of the network bandwidth. To address the problem, we propose a pipelined storage-based scatter-reduce method that simultaneously utilizes downlink and uplink bandwidth. Fig. 4(a) displays the state-of-the-art storage-based scatter-reduce method proposed in LambdaML [27]. It utilizes the computation resource of all workers for gradient aggregation by dividing the gradients as n splits, where n is the number of workers, and each worker is in charge of merging one split. The scatter-reduce process can be divided into three phases: in *phase 1*, each worker uploads the $n - 1$ gradient splits that other worker are in charge of to the storage. In *phase 2*, the i -th worker retrieves all the i -th splits uploaded by other workers and computes the merged gradients. In *phase 3*, each worker uploads its merged split and retrieves all other merged splits. The communication time of *phase 1* and *phase 2* are both $\frac{s_{grad}(n-1)}{n \cdot w} + t_{lat}$, where s_{grad} is the size of the gradients, w is the bandwidth of a worker and t_{lat} is the latency for accessing the storage. The communication time of *phase 3* is $\frac{s_{grad}}{w} + 2t_{lat}$, and the total synchronization time is

$$3 \cdot \frac{s_{grad}}{w} - \frac{2s_{grad}}{n \cdot w} + 4t_{lat} \quad (1)$$

As the upload in *phase 1* and the download in *phase 2* are performed in a serial fashion, the network resource is not efficiently utilized.

Our design further pipelines *phase 1* and *phase 2* to improve communication efficiency. The pipelined phase includes a total of n steps, as shown in Fig. 4(b):

- In step 1: worker i uploads gradient split $i + 1$ to storage.
- In step k , for $2 \leq k \leq n - 1$: worker i uploads gradient split $i + k$ to storage while downloading split i uploaded by worker $i - (k - 1)$.
- In step n : worker i downloads gradient split i uploaded by worker $i + 1$.

We use arithmetic modulo n in the above. The communication time of each of the above steps is $\frac{s_{grad}}{n \cdot w} + t_{lat}$, and the total time for n steps is $\frac{s_{grad}}{w} + n \cdot t_{lat}$. The synchronization time after pipelining is

$$2 \cdot \frac{s_{grad}}{w} + (2 + n)t_{lat} \quad (2)$$

Comparing (2) and (1), the pipelined scatter-reduce can achieve noticeable reduction in the transfer time, i.e. from $3 \frac{s_{grad}}{w} - \frac{2s_{grad}}{n \cdot w}$ to $2 \frac{s_{grad}}{w}$. For example, for an AWS Lambda function with 70MB/s bandwidth, the data transfer time in synchronizing a 280MB model among 8 workers can be reduced by 27%, from 11s to 8s. Although our design can suffer higher latency with the increase of workers, the latency is much smaller compared with the data transfer time, e.g. the measured t_{lat} is less than 40ms for AWS Lambda.

3.4 Co-optimization of Model Partition and Resource Allocation

In order to make the training pipeline fast and cost-efficient, we need to optimize the partition plan that splits model layers into different pipeline stages, and the resource allocation for each stage, including the number of workers used for intra-stage data parallelism as well as the memory size of each worker. A major challenge here is the strong coupling between model partitioning and resource allocation, which defies most existing solutions that optimize only one aspect [14, 38, 51]. In this section, we formulate the co-optimization of model partition and resource allocation as a mixed-integer quadratic program.

3.4.1 Formulation of Optimization Problem

Consider a model with L layers. Let $\mathcal{D} = \{D_1, \dots, D_K\}$ be the set of possible degrees of data parallelism, where $D_1 = 1$, meaning no data parallelism. Let $\mathcal{M} = \{M_1, \dots, M_J\}$ be the set of different memory sizes for serverless workers. We use a binary variables x_i to indicate whether the model is partitioned after layer i . Let $d \in \mathcal{D}$ be the degree of data parallelism. We enforce the same degree of data parallelism for all stages to reduce the problem complexity. Let $m_i \in \mathcal{M}$ be the memory size of workers holding layer i . We parameterize d and m_i as $d = \sum_{k=1}^K y_k D_k$ and $m_i = \sum_{j=1}^J z_{i,j} M_j$ with binary variables

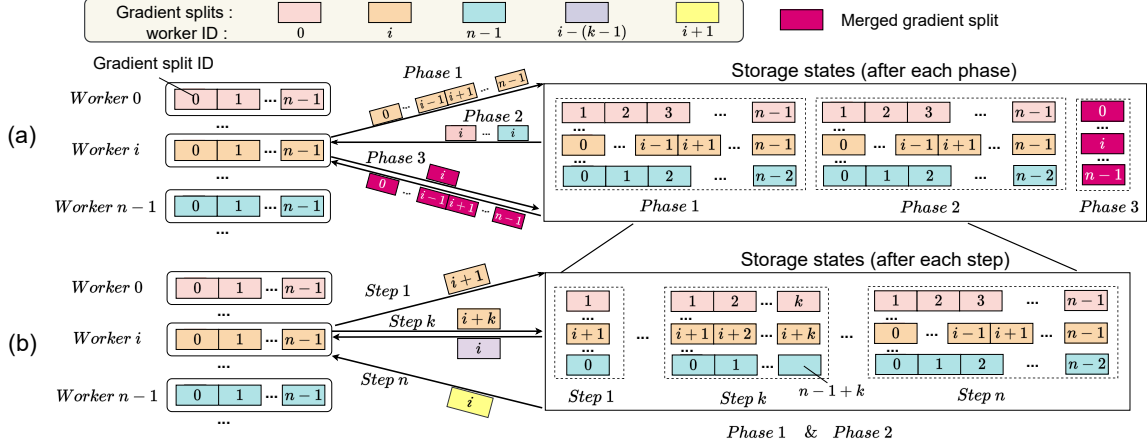


Figure 4: **Pipelined scatter-reduce.** (a) The scatter-reduce in LambdaML [27] has three phases where download and upload are performed in a serial fashion. (b) Our pipelined scatter-reduce performs download and upload in duplex in *phase 1* and *phase 2*.

y_k and $z_{i,j}$, where $y_k = 1$ if $d = D_k$ and $z_{i,j} = 1$ if $m_i = M_j$. The number of micro-batches per worker given by $\mu = \frac{M}{d} = \sum_{k=1}^K y_k \frac{M}{D_k}$, where M is the total number of micro-batches. Other notations will be introduced as needed; see Appendix A for a table of notations.

Our goal is to choose (x_i) , (y_k) and $(z_{i,j})$ to minimize the training cost c_{iter} and training time t_{iter} per iteration. We formulate it as the *nonlinear binary integer program* in (3), which we explain below.

$$\min \quad \alpha_1 \cdot c_{iter} + \alpha_2 \cdot t_{iter} \quad (3a)$$

$$s.t. \quad \mu \hat{a}_i + \hat{s}_i(4 - 2y_1) + s_0 \leq m_i, \quad 1 \leq i \leq L; \quad (3b)$$

$$|m_i - m_{i-1}| \leq x_{i-1} \cdot M_{\max}, \quad 2 \leq i \leq L; \quad (3c)$$

$$\sum_{k=1}^K y_k = 1, \quad \sum_{j=1}^J z_{i,j} = 1, \quad 1 \leq i \leq L; \quad (3d)$$

$$x_i, y_k, z_{i,j} \in \{0, 1\}, \quad \forall i, j, k. \quad (3e)$$

The expressions for c_{iter} and t_{iter} will be given in § 3.4.2. Note that we combine the two objectives into a single objective in (3a) using the weighted sum method. Each pair of weights (α_1, α_2) yields a Pareto optimal solution. As we vary the weights, the solutions will trace out the Pareto Frontier [39].

To explain the constraints, we first introduce the hat operator. Given any sequence u_1, u_2, \dots, u_L where u_i is a quantity associated with layer i , we define

$$\hat{u}_1 = u_1, \quad \hat{u}_i = u_i + \hat{u}_{i-1}(1 - x_{i-1}), \quad 2 \leq i \leq L, \quad (4)$$

where x_i are our decision variables for model partition. Let \mathcal{H} denote set of the highest layers of the partitions. For $i \in \mathcal{H}$, \hat{u}_i is the sum of the quantity u_j over the partition containing layer i . For the example in Fig. 3, $\mathcal{H} = \{1, 3, 4\}$ in Fig. 3 and $\hat{u}_3 = u_2 + u_3$ is the sum over partition 2.

The constraints (3b) specify that the memory consumption of each partition does not exceed the allocated memory of the corresponding worker. Let s_i denote the parameter size and a_i the activation size per micro-batch at layer i . For $i \in \mathcal{H}$, $\mu \hat{a}_i$ is the memory for activations of μ micro-batches in the partition that layer i belongs to; $\hat{s}_i(4 - 2y_1)$ comprises three parts of memory consumption, \hat{s}_i for parameters, \hat{s}_i for gradients, and $2(1 - y_1)\hat{s}_i$ for serialized data during model synchronization. Note synchronization is needed only if $y_1 = 0$. s_0 is the basic memory consumption of a serverless worker. e.g. memory consumed by the framework. We actually only need the constraints for $i \in \mathcal{H}$, as the others are redundant.

The constraints (3c) enforce consistency of the memory allocation for adjacent layers if they belong to the same partition, as they actually share the same workers, i.e. $m_i = m_{i-1}$ if $x_{i-1} = 0$. With $M_{\max} = \max_{1 \leq j \leq J} M_j$ being the maximum memory available, the constraint for i becomes vacuous when the model is partitioned after $i - 1$, i.e. $x_{i-1} = 1$.

The constraints (3d) and (3e) specify that we choose exactly one degree of data parallelism, and exactly one memory configuration for each layer.

To solve (3), we convert the formulation into an MIQP with common linearization techniques, which can then be solved by off-the-shelf solvers, e.g. Gurobi [18]. The details for linearization is in Appendix C.

3.4.2 Performance Model

Iteration cost. Recall the memory allocated for layer i workers is $m_i = \sum_{j=1}^J z_{i,j} M_j$. Since layers of the same partition are assigned to the same workers, we only count the layers in \mathcal{L} , and the total memory of all workers is

$$c_{mem} = d \sum_{i \in \mathcal{H}} m_i = d \left(\sum_{i=1}^{L-1} x_i m_i + m_L \right) \quad (5)$$

```

# Step1: get input training configurations
batch_size = int(event['batch_size'])
loss_func = ...
...

# Step2: build user-defined model and dataloader (Pytorch code)
model = ...
data_loader = ...

# Step3: wrap the model with FuncPipe API
Platform.use(platform_type) # Choose serverless platform
model = FuncPipe(model, loss_func=loss_func, ...) # Config training
model.init(event) # Initialize pipeline

# Step4: start training
for epoch_id in range(epochs):
    for batch_id, (inputs, targets) in enumerate(data_loader):
        model.pipeline.train(inputs, targets)

```

Figure 5: A **FUNCPipe** function example. Minimal changes to Pytorch training code are required (highlighted in orange).

The cost of serverless functions is proportional to the product of their running time and memory allocation, so the iteration cost c_{iter} is

$$c_{iter} = P \cdot t_{iter} \cdot c_{mem} \quad (6)$$

where P is the unit price specified by the service provider.

Iteration time. As shown in Fig. 3, the iteration time t_{iter} is given by

$$t_{iter} = t_f + \max_{1 \leq i \leq L} (t_b^i + t_s^i), \quad (7)$$

where t_f is the forward time. When layer i is the lowest layer of a partition (e.g. layer 2 in Fig. 3), t_b^i is the computation completion time of that partition, and t_s^i the corresponding model synchronization time. For other layers (e.g. layer 3 in Fig. 3), t_b^i and t_s^i are defined in (11) and (12) without the above interpretations; their sum $t_b^i + t_s^i$ will be dominated by that of the lowest layer of the same partition (e.g. layer 2), and hence their inclusion in (7) does not affect t_{iter} . The detailed calculation of each term is in Appendix B.

4 Implementation

FUNCPipe is implemented on top of *Pytorch* with more than 4000 lines of Python code. As shown in Fig. 5, it provides easy-to-use APIs and requires minimal changes (highlighted) to legacy training code on the user side. FUNCPipe currently supports two serverless platforms, AWS Lambda and Alibaba Cloud Function Compute, and can be easily extended to other platforms as the platform API design in FUNCPipe is decoupled from the underlying SDK implementations, e.g. *boto3* for AWS Lambda and *fc2* for Alibaba Cloud Function Compute.

Pipeline Task Overlap. The different tasks, *upload*, *download*, and *computation* have internal dependencies and different resource requirements, i.e., download bandwidth, uplink bandwidth, and CPU. These tasks are organized as Directed

Acyclic Graphs (DAGs) and handled by different threads in the *Task Executor*. Tasks of different types are processed in parallel; each of them is assigned a unique ID and contains a set of IDs representing its dependencies. A task is immediately processed once its dependencies are satisfied.

Communication Collectives. FUNCPipe performs storage-based communications, including *send-and-recv* between different partitions and *scatter-reduce* among partition replicas. The data communicated are serialized with the python library *pickle* and uploaded to the storage bucket as files. Meta-data information is included in the file name to distinguish different pairs and types of communication. Workers periodically query the cloud storage bucket to check for *download*.

MIQP Solution. For models with over a hundred layers, solving the MIQP problem can take hours or even days, limiting its practical usage. As many model layers can have small memory consumption and short computation time, they can be merged with other layers to reduce the value of L , i.e. the total number of layers in optimization. By merging the layers, our method ensures a minute-level solution time. Currently, we provide three options for the merging criterion, computation time, parameter size, or activation size. For all the tested models, merging by balancing the computation time achieves better performance and is adopted in our experiments.

FUNCPipe provides two implementations for *Partition/Resource Optimizer*. The first one solves the MIQP optimization using serverless functions. However, off-the-shelf solvers can have licence limits that require additional support in order to be used in the serverless environment. For example, Gurobi requires user to have a Gurobi token server that grants temporary license [19]. For users that want to avoid such effort, we provide a second implementation that solves the MIQP optimization at the client side. The information obtained by *Model Profiler* is retrieved by the client for optimization and the results are uploaded back to the initial worker.

Limitation Discussion. Currently FUNCPipe does not support training models with a large layer that exceeds the maximum memory for a serverless function. One way to support such models is to further partition at the tensor level, i.e., tensor parallelism [26, 47, 48]. Extending FUNCPipe to tensor parallelism is left for future work.

5 Evaluation

In this section we first evaluate the overall performance of FUNCPipe by comparing it with state-of-the-art serverless-based training designs (§ 5.2) and discuss its system scalability (§ 5.4). We then validate the effectiveness of its designs with component-wise study, including the performance evaluation of our pipelined scatter-reduce (§ 5.5) and co-optimization of model partition and resource allocation (§ 5.6). Finally, we conclude the evaluation by discussing the effect of resource availability on different serverless platforms (§ 5.7).

Model name	Parameter size (MB)	Activation size per sample (MB)
ResNet101	170	198
AmoebaNet-D18	476	432
AmoebaNet-D36	900	697
BERT-Large	1153	263

Table 1: **Models used for evaluation.** *AmoebaNet-D18* and *AmoebaNet-D36* are two *AmoebaNet-D* models with 18 and 36 normal cell layers, respectively. Both have filter size 256.

5.1 Methodology

Testbed. Our evaluation uses two of the mainstream serverless platforms, AWS Lambda [5] and Alibaba Cloud Function Compute [2], that provide different resource options. AWS Lambda provides a maximum of 10 GBytes memory allocation for each serverless function. Its corresponding cloud storage service, S3, grants unlimited bandwidth to concurrent access. Alibaba Cloud Function Compute has different resource availability compared with AWS Lambda. It allows a maximum memory allocation of 32 Gbytes and its cloud storage OSS puts a limit on the concurrent bandwidth, e.g. a total of 10Gb/s for a normal user. Our evaluation is mainly performed on AWS Lambda and we evaluate FUNCPIPE on Alibaba Cloud Function Compute to discuss the effect of resource availability on different serverless platforms.

Models and Datasets. The DL models used for our evaluation are displayed in Table 1. *ResNet101*, *AmoebaNet-D18*, and *AmoebaNet-D36* are popular Convolution Neural Network (CNN) models for computer vision tasks. *BERT-Large* is a transformer model for natural language processing. We use the popular image classification dataset *CIFAR-10* to train the CNN models. To train *BERT-Large*, we run masked language modeling on the dataset *Wikitext-2*. We use synchronous Stochastic Gradient Descent (SGD) optimizer with the same global batch size (further explained in § 5.2) for all tested designs in the evaluation, and we report the average per-iteration training time and cost.

Baselines. We compare FUNCPIPE with existing serverless-based training designs with two different structures: the pure serverless-based structure and the hybrid PS structure (as introduced in § 2.2). LambdaML [27] is the state-of-the-art pure serverless-based training framework and it also includes an implementation of the hybrid design exemplified by Cirrus [9]. The two implementations are referred to as *LambdaML* and *HybridPS*. Their default resource strategy uses the maximum memory allocation and maximum local batch size within the memory limit for each worker. We further integrate *gradient accumulation* into the two implementations, referred to as *LambdaML-GA* and *HybridPS-GA*. Gradient accumulation is a commonly adopted technique used for reducing the

memory consumption in training [12, 49, 50]. LambdaML-GA and HybridPS-GA use the same number of workers as LambdaML and HybridPS but allocate *the minimum memory* required after performing gradient accumulation for each worker. LambdaML-GA and HybridPS-GA serve as baselines with reduced worker memory allocation and better balanced computation to communication time ratio.

To validate the effectiveness of our co-optimization on model partition and resource allocation, we compare with the existing algorithms *TPDMP* and *Bayes*. TPDMP is the latest graph-based model partition algorithm [51] developed for server-based pipeline training, it optimizes model partition on a fixed set of workers/resources. We perform a grid search on the resource allocation and optimizes the model partition with TPDMP for each allocation. We select the configuration that minimizes the objective function in (3). Bayes is a blackbox optimization method that has been proved effective in deciding configurations for cloud services [4]. It can jointly optimize model partition and resource allocation. Further details of the baselines are explained in Appendix D.

FUNCIPIE Settings. For the evaluation, we use 8 discrete memory allocation choices, i.e., [512MB, 1024MB, 2048MB, 3072MB, 4096MB, 6144MB, 8192MB, 10240MB]. We empirically set the micro-batchsize to 4 as it achieves a generally better performance on the evaluation models. We use four pairs of weights of (α_1, α_2) , i.e. [(1, 0), (1, 2¹⁶), (1, 2¹⁹), (1, 2²²)], to locate the corresponding points on the Pareto Frontier. The same pairs of weights are used for the baseline algorithm TPDMP and Bayes.

Recommendation. FUNCPIPE also recommends a configuration out of the optimized results. Denote the training time and cost of the cheapest configuration, i.e., configuration that optimizes only for cost, as t_{cost} and c_{cost} , and the training time and cost of another configuration as t_p and c_p . We use $\delta = (t_{cost}/t_p - 1)/(c_p/c_{cost} - 1)$ to represent how efficient a configuration is by comparing its speedup with its cost increase over the cheapest configuration. In our evaluation FUNCPIPE recommends the fastest configuration that satisfies $\delta \geq 0.8$.

5.2 Overall Performance

The training performance of FUNCPIPE and its comparison with existing serverless-based training designs are shown in Fig. 6 and Fig. 7. Generally, FUNCPIPE achieves better performance in both training speed and cost over existing designs in most of the test cases (comparable or faster performance in other cases). And the performance improvement increases with the model size and global batch size. The results are obtained with three commonly adopted global batch size of 16, 64 and 256. The performance of each baseline method is represented as a single point in the figure, and for FUNCPIPE it is a curve consisting of the points corresponding to the configurations obtained using the four pairs of weights. Note

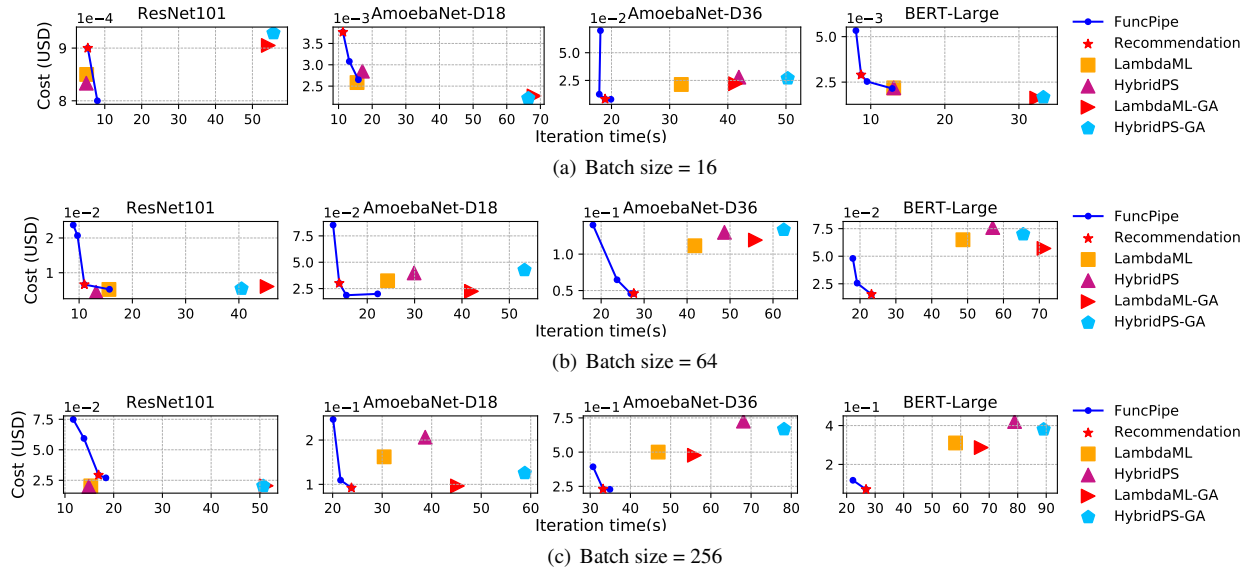


Figure 6: **Overall training performance.** FUNCPIPE outperforms existing designs in both training speed and cost in most of the test cases, and achieves comparable or faster performance in other cases.

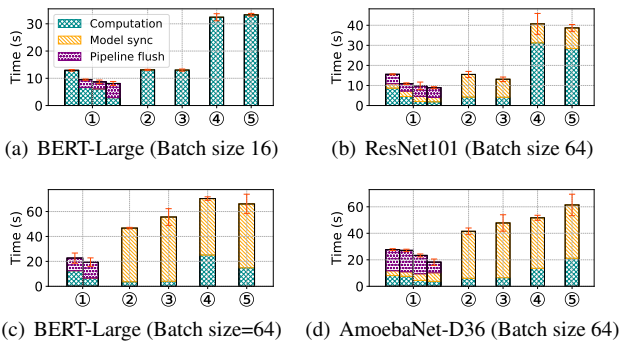


Figure 7: **Training time breakdown.** Labels: ①FUNCPIPE, ②LambdaML, ③HybridPS, ④LambdaML-GA, ⑤HybridPS-GA. The multiple bars of FUNCPIPE correspond to different configurations on the Pareto Frontier. Legend shared across figures.

that there can be less than four points on a curve as different weights can lead to the same configuration. The configuration recommended by FUNCPIPE is also highlighted in this figure. We make the following key observations.

First, when the global batch size is small and that training on a single worker is feasible, FUNCPIPE can achieve up to 1.6x speedup over the best-performing serverless-based training baseline (LambdaML) when given more resources (2.4x cost). Although existing designs can achieve similar cost-efficient training to FUNCPIPE, their training speed can not be improved giving more resource, as further illustrated by the time breakdown in § 5.3.

Second, FUNCPIPE achieves an average of **1.7X** training

speedup and **53%** cost reduction compared with the best-performing baseline LambdaML when training *AmoebaNet-D18*, *AmoebaNet-D36* and *BERT-Large* with global batch sizes of 64 and 256, with up to **2.2X** speedup and **77%** cost reduction when training *BERT-Large* with global batch size 256. The improved training speed and cost-efficiency come from the reduced communication time and increased computation to communication ratio, as further illustrated in § 5.3.

Third, the hybrid design, HybridPS, achieves comparable or even better performance than LambdaML when training *ResNet101*. However, with the increase of model size and global batch size (leading to the use of more workers), the server node in this centralized structure can be heavily burdened. As a result, we can observe noticeable performance gap between HybridPS and LambdaML when training *AmoebaNet-D36* and *BERT-Large* in Fig. 6(c). In addition, we see that the use of gradient accumulation (LambdaML-GA and HybridPS-GA) can reduce the training cost at the price of a longer training time. However, the reduction is neither significant nor guaranteed to exist. We attribute it to that the use of gradient accumulation reduces the memory allocation but the increased runtime raises the cost.

5.3 Training Time Breakdown

Fig. 7(a) displays the time breakdown for the training of *BERT-Large* in Fig. 6(a). The small batch size allows the baseline methods to train the model on a single worker (no communication time), and thus fully utilize the computation resource and achieve cost-efficient training. However, their training speed cannot be improved any further. As their work-

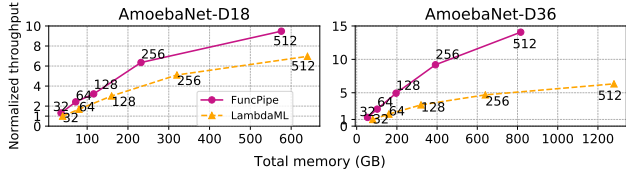


Figure 8: **System scalability test.** FUNCPIPE achieves higher throughput and is more robust to bandwidth contention. Each data point is annotated with the global batch size.

ers already have the maximum memory allocation, increasing the resource usage means using more workers. Such scaling up incurs high communication cost and stalls the training—synchronizing *BERT-Large* (1153MB) with 70MB/s bandwidth can take ten of seconds, which is longer the total computation time. This shows that FUNCPIPE can be faster than existing designs even when training with small batch size.

Fig. 7(b) shows the time breakdown of training *ResNet101* with batch size = 64 (i.e., Fig. 6(b)). The improvement in training speed achieved by FUNCPIPE is relatively smaller compared to that in Fig. 7(c) and Fig. 7(d). This is because when the model size is small, the synchronization time of LambdaML and HybridPS can be close to the sum of pipeline flush time and intra-stage model synchronization time in FUNCPIPE. This suggests that with small-sized models, we expect small improvement or comparable performance from FUNCPIPE.

Fig. 7(c) and Fig. 7(d) show the time breakdown for training *BERT-Large* and *AmoebaNet-D36*, respectively (i.e., Fig. 6(b)). The breakdown explains the major performance improvement observed in Fig. 6. The improvement achieved by FUNCPIPE can be largely attributed to the reduced communication time, i.e., its pipeline flush time and intra-stage model synchronization time is much lower than the synchronization time of LambdaML. We can also see that FUNCPIPE has a larger computation to communication time ratio compared with the baseline methods, making FUNCPIPE more cost-efficient.

5.4 System Scalability

Next, we evaluate the scalability of FUNCPIPE by comparing its performance to the best-performing design, i.e., LambdaML, based on observations from § 5.2. For this experiment, we use the total amount of allocated memory to denote the system resource. Further, we use the global batch size to specify the amount of work. As such, we are evaluating both FUNCPIPE and LambdaML’s ability to handle more work (i.e., increased global batch size) given more resource (i.e., total memory). For LambdaML, we increase the global batch size and resource usage by adding more workers. Each worker is allocated the maximum memory and uses the maximum local batch size according to the resource strategy of LambdaML.

For FUNCPIPE, we increase the global batch size and use the recommended configuration.

Fig. 8 reports the average training throughput, i.e., number of processed samples per second, on model *AmoebaNet-D18* and *AmoebaNet-D36*. The training throughput is normalized to that of LambdaML with global batch size 32. We first observe that FUNCPIPE achieves higher training throughput than LambdaML when given the same resource allocation. For example, when training the *AmoebaNet-D36* model, the throughput is estimatedly 180% higher when both given 800 GB total memory. Second, both FUNCPIPE and LambdaML exhibit a non-linear scaling up performance with FUNCPIPE scales better with the total memory and the global batch size. We find that the per-worker network bandwidth reduction contributes to the scaling up performance. The per-worker bandwidth reduction was also observed in prior work [53], and we suspect that it is due to the serverless platforms schedule different serverless functions to machines that share the bandwidth capacity. Additionally, we see that FUNCPIPE is less impacted by the bandwidth reduction than LambdaML, possibly due to the effectiveness of FUNCPIPE’s designs in reducing the overall communication burden.

5.5 Scatter-reduce Communication Efficiency

We compare our pipelined scatter-reduce design with LambdaML’s scatter-reduce [27]. The results show that our design reduces the synchronization time by up to 26% and improves the training throughput by 22% (18% reduction in iteration time). To perform the comparison, we use the recommended configuration for training *AmoebaNet-D18* with a global batch size 32. The configuration divides the model into three stages and each stage has a data parallelism of two. We gradually increase the level of data parallelism (the global batch size is increased proportionally) from two to 32, and compares the training throughput. As shown in Fig. 9(a), the two scatter-reduce methods achieve similar performance with small data parallel levels at the beginning. As the data parallel level increases, we observe a growing performance gap and our pipelined scatter-reduce design achieves a 22% higher training throughput than LambdaML’s scatter-reduce. This increased performance gap can be understood in two ways. First, the increased data parallelism level will increase the difference in transfer time of the two algorithms; this can be seen by comparing (1) and (2). Theoretically, a reduction of up to 33% in transfer time can be achieved. In Fig. 9(b), we show that the gap between the synchronization time gradually increases and can reach 26%. Second, the increased data parallelism level requires the use of more workers. Based on our observation in AWS Lambda, more workers can reduce the available bandwidth per worker. As such, the communication time can take up a larger proportion of the overall training time, thus emphasizing the critical role of and the benefit of our co-optimization. In summary, our pipelined scatter-reduce

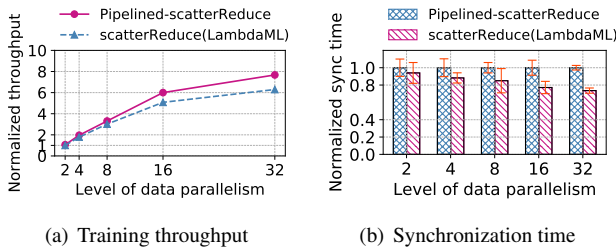


Figure 9: **Performance of our pipelined scatter-reduce method.** Our design achieves up to 22% higher training throughput and 26% lower synchronization time.

can effectively improve communication efficiency.

5.6 Co-optimization Performance

We evaluate the performance of our co-optimization design by comparing with existing model partition/resource allocation algorithms in two major aspects, training performance and solution time cost.

Training Performance. Fig. 10 compares the model partition and resource allocation policies found by our co-optimization method and those by two existing algorithms [8, 51]. Note that some methods in the figure contain less points as they generate the same configuration for different pairs of weights. The results show that our design achieves the best overall performance. Compared to *TPDMP*, our design has a comparable average training cost (within 3% difference) but an average speedup of **1.8X** when optimized for the same objective function. The performance gap between our design and *TPDMP* suggests the benefit of co-optimizing the model partition and resource allocation. Compared to *Bayes*, our co-optimization method achieves **7%** higher average training speed and **55%** lower average cost. We observe that the policies generated by *Bayes* often have higher monetary costs; we attribute *Bayes*’s cost-inefficiency to its tendency of over-provisioning the resource to avoid infeasible solutions, i.e., policies that lead to OOM error. We also evaluate the accuracy of the performance model to validate the effectiveness of our formulation. Results show that our model achieves an average prediction error of less than **12%**. See Appendix E for further details.

Solution Time Cost. We evaluate the algorithms on the client side using an *Intel(R) Core(TM) i5-10210U CPU*. The average solution time for each configuration in Fig. 10 is **274s**, **603s**, **45s** for FUNCPIPE, TPDMP and Bayes respectively. The results show that FUNCPIPE achieves the best performance with a reasonable, i.e. minute level, solution cost.

5.7 Impact of Different Resource Availability

We lastly evaluate the performance of FUNCPIPE on the Alibaba Cloud to understand the potential impact of different

resource availability. The major difference between AWS and Alibaba cloud is that the bandwidth of Alibaba Cloud storage OSS [3], has a limit of 10Gb/s. The same bandwidth limit is with the VM instance used by the HybridPS baseline. We study how the same bandwidth bottleneck effect the performance of these methods. Due to the space limitation, we only display the results of training *ResNet101* and *AmoebaNet-D36* with global batch size 64 and 256 in Fig. 11. Overall, we find that FUNCPIPE demonstrates similar benefits in Alibaba Cloud to AWS: comparable performance or small improvement on small-sized models and better performance in both training speed and cost as the model size and global batch size increase, with up to **1.8X** speedup and **49%** cost reduction compared with the best-performing baseline HybridPS. Such performance benefits are attributed to the key designs of FUNCPIPE, including the use of model partition technique, efficient scatter-reduce design, and the co-optimization of partition and resource allocation policy; FUNCPIPE can greatly reduce the communication burden in training and thus alleviate the effect of the limited bandwidth.

Other platforms [36] may have similar limit on the storage bandwidth, e.g. Azure Storage has a total limit of 25Gb/s [37]. Such bandwidth bottleneck may limit the ability of FUNCPIPE to scale out, and FUNCPIPE may eventual be outperformed by HybridPS as the bandwidth of HybridPS can be increased by scaling up the parameter server. One solution for this is to use VM-based storage design, like Pocket [29], and the bandwidth can be increased the same way as HybridPS. In such case we expect FUNCPIPE to achieve better performance than HybridPS, as the evaluation has demonstrated the performance benefits of FUNCPIPE with the same available bandwidth. Extending FUNCPIPE to VM-based storage and further comparing to the HybridPS design is left as future work.

6 Related Work

Pipeline in Serverless-based Training. To the best of our knowledge, Dorylus [53] is the only existing work that combines the notion of pipeline and serverless-based training. Dorylus is specialized for Graph Neural Network (GNN) models and adopts a hybrid system structure, i.e., CPU servers with serverless functions. It exploits the inherent features of GNN to separate the computation tasks, and uses serverless functions only for the lightweight linear algebra operations. Its pipeline design focuses on overlapping the computation tasks on server and serverless functions to hide network latency. Our work, on the other hand, exploits serverless-based pipeline for training DNN models. Our tasks cannot be easily separated and trained the same way as GNNs as they require much heavier computation and communication on serverless functions. We address such challenges with efficient communication design and careful co-optimization of model partition and resource allocation.

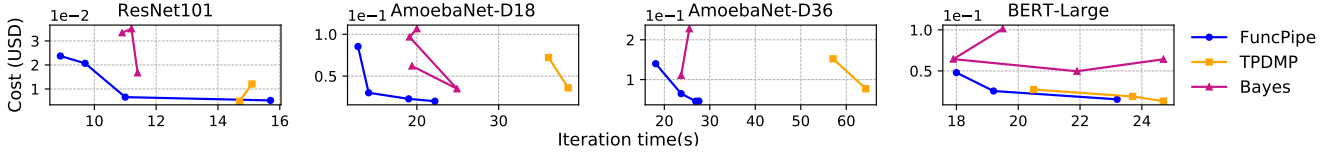


Figure 10: **Co-optimization performance evaluation.** The global batch size is 64. Other batch sizes are similar.

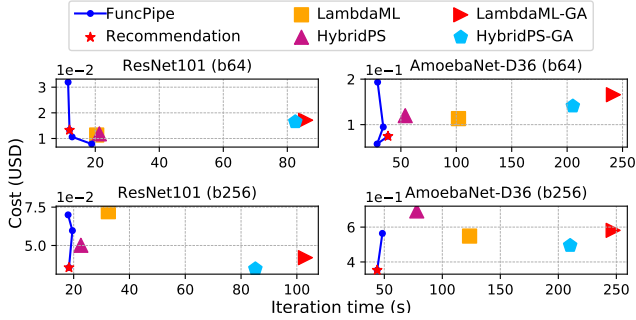


Figure 11: **Training performance on Alibaba Cloud.** With the same limit on total communication bandwidth, FUNCPIPE achieves up to **1.8X** speedup and **49%** cost reduction compared with the best-performing baseline HybridPS.

Serverless Communication. Feng et al. [15] proposes two centralized storage-based methods for model synchronization. However, such design is generally of low efficiency due to the bandwidth bottleneck of the central nodes. LambdaML proposes a more efficient decentralized scatter-reduce method but it fails to fully utilize the available bandwidth [27]. In parallel, other works focus on improving the performance of storage system for higher communication efficiency. Pocket proposes a distributed data store that provides better elasticity and latency [29]. Shredder designs a low-latency cloud store that supports in-storage computing [62]. Such designs and optimizations are orthogonal to our pipelined storage-based communication approach. Another choice is to use common *NAT-traversal* techniques to enable direct communication among functions [16, 59]. The direct communication can allow existing communication designs, e.g., ringAllreduce [43], to be used. However, NAT-traversal usually requires external servers that can cause communication bottleneck. The performance of using existing communication designs for serverless-based training with NAT-traversal remains unclear.

Model Partition and Resource Allocation in Serverless. Recent works have studied the model partition and resource allocation problem for serverless-based inference serving [24, 61]. These works aim at satisfying Service Level Objectives in latency while minimizing cost or further improving throughput. Gillis fixes the per-function memory allocation and optimizes model partition to lower inference cost with a reinforcement learning approach [61]. AMPS fixes

the number of functions/partitions and co-optimizes the partition and memory allocation with an MIP formulation [24]. Compared with inferencing, training has a different and more complex process and it requires new formulation. Its optimization includes more decision factors such as inter-stage data parallelism and synchronization cost, thus it faces more challenges in generating efficient model partition and resource configuration. For example, both the number of functions and the number of partitions require co-optimization with memory allocation.

7 Conclusion

In this paper, we presented the design and implementation of the first pipelined serverless training framework called FUNCPIPE. With the ever increasing interests in truly taking advantage of serverless computing, many researchers have looked at utilizing serverless functions to build scalable applications and improving serverless platforms [44, 45, 53, 55]. Our key goal can be simply boiled down to understand *how to allow DL practitioners to train models on serverless platforms* in a fast and low-cost manner, regardless of model size and training hyperparameters such as batch size that impact memory consumption. Moreover, we wanted FUNCPIPE to be an entirely serverless framework to fully enjoy various benefits of serverless, in contrast to previously proposed hybrid design of leveraging VMs [9, 60].

With three key designs—(i) the pipeline parallelism for model partitions, (ii) the communication-efficient scatter-reduce, and (iii) the co-optimization of partition and resource allocation policy, FUNCPIPE was able to overcome the current limitations of serverless platforms (e.g., relatively low memory and bandwidth capacity compared to model training). The benefits of FUNCPIPE, tested with four commonly used models and on two popular serverless providers in numerous settings, are up to **2.2X** training speedup and **77%** cost reduction compared to state-of-the-art serverless training frameworks [27]. We carefully untangled the benefits with in-depth component breakdown analysis and showed both (ii) and (iii) designs outperformed their counterparts. We concluded that FUNCPIPE demonstrates a promising design for training DL models on current serverless platforms; as part of future work, we would like to explore other techniques such as tensor parallelism to further improve FUNCPIPE’s performance.

References

- [1] Istemi Ekin Akkus, Ruichuan Chen, Ivica Rimac, Manuel Stein, Klaus Satzke, Andre Beck, Paarijaat Aditya, and Volker Hilt. SAND: Towards High-Performance Serverless Computing. In *2018 Usenix Annual Technical Conference (USENIX ATC 18)*, pages 923–935, 2018.
- [2] Alibaba. Alibaba cloud function compute. <https://www.aliyun.com/product/fc>.
- [3] Alibaba. Alibaba cloud object storage service. <https://www.aliyun.com/product/oss>.
- [4] Omid Alipourfard, Hongqiang Harry Liu, Jianshu Chen, Shivaram Venkataraman, Minlan Yu, and Ming Zhang. CherryPick: Adaptively unearthing the best cloud configurations for big data analytics. In *14th USENIX Symposium on Networked Systems Design and Implementation (NSDI 17)*, pages 469–482, 2017.
- [5] Amazon. Aws lambda. <https://aws.amazon.com/lambda/>.
- [6] Ammar Ahmad Awan, Arpan Jain, Quentin Anthony, Hari Subramoni, and Dhabaleswar K Panda. Hyparflow: Exploiting mpi and keras for scalable hybrid-parallel dnn training using tensorflow. *arXiv preprint arXiv:1911.05146*, 2019.
- [7] Zhengda Bian, Qifan Xu, Boxiang Wang, and Yang You. Maximizing parallelism in distributed training for huge neural networks. *arXiv preprint arXiv:2105.14450*, 2021.
- [8] Eric Brochu, Vlad M Cora, and Nando De Freitas. A tutorial on bayesian optimization of expensive cost functions, with application to active user modeling and hierarchical reinforcement learning. *arXiv preprint arXiv:1012.2599*, 2010.
- [9] Joao Carreira, Pedro Fonseca, Alexey Tumanov, Andrew Zhang, and Randy Katz. Cirrus: A serverless framework for end-to-end ml workflows. In *Proceedings of the ACM Symposium on Cloud Computing*, pages 13–24, 2019.
- [10] Chi-Chung Chen, Chia-Lin Yang, and Hsiang-Yun Cheng. Efficient and robust parallel dnn training through model parallelism on multi-gpu platform. *arXiv preprint arXiv:1809.02839*, 2018.
- [11] Ching-Hsiang Chu, Pouya Kousha, Ammar Ahmad Awan, Kawthar Shafie Khorassani, Hari Subramoni, and Dhabaleswar K Panda. Nv-group: link-efficient reduction for distributed deep learning on modern dense gpu systems. In *Proceedings of the 34th ACM International Conference on Supercomputing*, pages 1–12, 2020.
- [12] Aditya Devarakonda, Maxim Naumov, and Michael Garland. Adabatch: Adaptive batch sizes for training deep neural networks. *arXiv preprint arXiv:1712.02029*, 2017.
- [13] Simon Eismann, Joel Scheuner, Erwin Van Eyk, Maximilian Schwinger, Johannes Grohmann, Nikolas Herbst, Cristina L Abad, and Alexandru Iosup. Serverless applications: Why, when, and how? *IEEE Software*, 38(1):32–39, 2020.
- [14] Shiqing Fan, Yi Rong, Chen Meng, Zongyan Cao, Siyu Wang, Zhen Zheng, Chuan Wu, Guoping Long, Jun Yang, Lixue Xia, et al. Dapple: A pipelined data parallel approach for training large models. In *Proceedings of the 26th ACM SIGPLAN Symposium on Principles and Practice of Parallel Programming*, pages 431–445, 2021.
- [15] Lang Feng, Prabhakar Kudva, Dilma Da Silva, and Jiang Hu. Exploring serverless computing for neural network training. In *2018 IEEE 11th international conference on cloud computing (CLOUD)*, pages 334–341. IEEE, 2018.
- [16] Sadjad Fouladi, Francisco Romero, Dan Iter, Qian Li, Shuvo Chatterjee, Christos Kozyrakis, Matei Zaharia, and Keith Winstein. From laptop to lambda: Outsourcing everyday jobs to thousands of transient functional containers. In *2019 USENIX Annual Technical Conference (USENIX ATC 19)*, pages 475–488, 2019.
- [17] Jinkun Geng, Dan Li, and Shuai Wang. Horizontal or vertical? a hybrid approach to large-scale distributed machine learning. In *Proceedings of the 10th Workshop on Scientific Cloud Computing*, pages 1–4, 2019.
- [18] Gurobi. Gurobi - the fastest solver. <https://www.gurobi.com>.
- [19] Gurobi. Setting up and using a floating license. https://www.gurobi.com/documentation/9.5/quickstart_mac/setting_up_and_using_a_floating_license.html.
- [20] Scott Hendrickson, Stephen Sturdevant, Tyler Harter, and Venkataramani. Serverless computation with OpenLambda. In *8th USENIX Workshop on Hot Topics in Cloud Computing (HotCloud 16)*, 2016.
- [21] Yanping Huang, Youlong Cheng, Ankur Bapna, Orhan Firat, Dehao Chen, Mia Chen, HyoukJoong Lee, Jiquan Ngiam, Quoc V Le, Yonghui Wu, et al. Gpipe: Efficient training of giant neural networks using pipeline parallelism. *Advances in neural information processing systems*, 32, 2019.

- [22] Arpan Jain, Ammar Ahmad Awan, Asmaa M Aljuhani, Jahanzeb Maqbool Hashmi, Quentin G Anthony, Hari Subramoni, Dhableswar K Panda, Raghu Machiraju, and Anil Parwani. Gems: Gpu-enabled memory-aware model-parallelism system for distributed dnn training. In *SC20: International Conference for High Performance Computing, Networking, Storage and Analysis*, pages 1–15. IEEE, 2020.
- [23] Arpan Jain, Ammar Ahmad Awan, Asmaa M Aljuhani, Jahanzeb Maqbool Hashmi, Quentin G Anthony, Hari Subramoni, Dhableswar K Panda, Raghu Machiraju, and Anil Parwani. Gems: Gpu-enabled memory-aware model-parallelism system for distributed dnn training. In *SC20: International Conference for High Performance Computing, Networking, Storage and Analysis*, pages 1–15. IEEE, 2020.
- [24] Jananie Jarachanthan, Li Chen, Fei Xu, and Bo Li. Amps-inf: Automatic model partitioning for serverless inference with cost efficiency. In *50th International Conference on Parallel Processing*, pages 1–12, 2021.
- [25] Zhihao Jia, Matei Zaharia, and Alex Aiken. Beyond data and model parallelism for deep neural networks. *Proceedings of Machine Learning and Systems*, 1:1–13, 2019.
- [26] Zhihao Jia, Matei Zaharia, and Alex Aiken. Beyond data and model parallelism for deep neural networks. *Proceedings of Machine Learning and Systems*, 1:1–13, 2019.
- [27] Jiawei Jiang, Shaoduo Gan, Yue Liu, Fanlin Wang, Gustavo Alonso, Ana Klimovic, Ankit Singla, Wentao Wu, and Ce Zhang. Towards demystifying serverless machine learning training. In *Proceedings of the 2021 International Conference on Management of Data*, pages 857–871, 2021.
- [28] Ana Klimovic, Yawen Wang, Christos Kozyrakis, Patrick Stuedi, Jonas Pfefferle, and Animesh Trivedi. Understanding ephemeral storage for serverless analytics. In *2018 USENIX Annual Technical Conference (USENIX ATC 18)*, pages 789–794, 2018.
- [29] Ana Klimovic, Yawen Wang, Patrick Stuedi, Animesh Trivedi, Jonas Pfefferle, and Christos Kozyrakis. Pocket: Elastic ephemeral storage for serverless analytics. In *13th USENIX Symposium on Operating Systems Design and Implementation (OSDI 18)*, pages 427–444, 2018.
- [30] Shen Li, Yanli Zhao, Rohan Varma, Omkar Salpekar, Pieter Noordhuis, Teng Li, Adam Paszke, Jeff Smith, Brian Vaughan, Pritam Damania, et al. Pytorch distributed: Experiences on accelerating data parallel training. *arXiv preprint arXiv:2006.15704*, 2020.
- [31] Shigang Li and Torsten Hoefler. Chimera: efficiently training large-scale neural networks with bidirectional pipelines. In *Proceedings of the International Conference for High Performance Computing, Networking, Storage and Analysis*, pages 1–14, 2021.
- [32] Shijian Li, Oren Mangoubi, Lijie Xu, and Tian Guo. Sync-switch: Hybrid parameter synchronization for distributed deep learning. In *2021 IEEE 41th International Conference on Distributed Computing Systems (ICDCS)*, 2021.
- [33] Shijian Li, Robert J. Walls, and Tian Guo. Characterizing and modeling distributed training with transient cloud gpu servers. In *2020 IEEE 40th International Conference on Distributed Computing Systems (ICDCS)*, 2020.
- [34] Ryan McDonald, Keith Hall, and Gideon Mann. Distributed training strategies for the structured perceptron. In *Human language technologies: The 2010 annual conference of the North American chapter of the association for computational linguistics*, pages 456–464, 2010.
- [35] Garrett McGrath and Paul R Brenner. Serverless computing: Design, implementation, and performance. In *2017 IEEE 37th International Conference on Distributed Computing Systems Workshops (ICDCSW)*, pages 405–410. IEEE, 2017.
- [36] Microsoft. Microsoft azure cloud computing. <https://azure.microsoft.com/>.
- [37] Microsoft. Microsoft azure storage. <https://azure.microsoft.com/services/storage>.
- [38] Deepak Narayanan, Aaron Harlap, Amar Phanishayee, Vivek Seshadri, Nikhil R Devanur, Gregory R Ganger, Phillip B Gibbons, and Matei Zaharia. Pipedream: generalized pipeline parallelism for dnn training. In *Proceedings of the 27th ACM Symposium on Operating Systems Principles*, pages 1–15, 2019.
- [39] Patrick Ngatchou, Anahita Zarei, and A El-Sharkawi. Pareto multi objective optimization. In *Proceedings of the 13th International Conference on, Intelligent Systems Application to Power Systems*, pages 84–91. IEEE, 2005.
- [40] Pitch Patarasuk and Xin Yuan. Bandwidth efficient all-reduce operation on tree topologies. In *2007 IEEE International Parallel and Distributed Processing Symposium*, pages 1–8. IEEE, 2007.
- [41] Pitch Patarasuk and Xin Yuan. Bandwidth optimal all-reduce algorithms for clusters of workstations. *Journal of Parallel and Distributed Computing*, 69(2):117–124, 2009.

- [42] Thomas Rausch, Waldemar Hummer, Vinod Muthusamy, Alexander Rashed, and Schahram Dustdar. Towards a serverless platform for edge AI. In *2nd USENIX Workshop on Hot Topics in Edge Computing (HotEdge 19)*, 2019.
- [43] Baidu Research. baidu-allreduce, 2017. <https://github.com/baidu-research/baidu-allreduce>.
- [44] Francisco Romero, Gohar Irfan Chaudhry, Íñigo Goiri, Pragna Gopa, Paul Batum, Neeraja J Yadwadkar, Rodrigo Fonseca, Christos Kozyrakis, and Ricardo Bianchini. FaaS\$: A Transparent Auto-Scaling Cache for Serverless Applications. 2021.
- [45] Francisco Romero, Mark Zhao, Neeraja J. Yadwadkar, and Christos Kozyrakis. Llama: A heterogeneous & serverless framework for auto-tuning video analytics pipelines. In *Proceedings of the ACM Symposium on Cloud Computing, SoCC '21*, 2021.
- [46] Christopher J Shallue, Jaehoon Lee, Joseph Antognini, Jascha Sohl-Dickstein, Roy Frostig, and George E Dahl. Measuring the effects of data parallelism on neural network training. *arXiv preprint arXiv:1811.03600*, 2018.
- [47] Noam Shazeer, Youlong Cheng, Niki Parmar, Dustin Tran, Ashish Vaswani, Penporn Koanantakool, Peter Hawkins, et al. Mesh-tensorflow: Deep learning for supercomputers. *Advances in neural information processing systems*, 31, 2018.
- [48] Mohammad Shoeybi, Mostafa Patwary, Raul Puri, Patrick LeGresley, Jared Casper, and Bryan Catanzaro. Megatron-lm: Training multi-billion parameter language models using model parallelism. *arXiv preprint arXiv:1909.08053*, 2019.
- [49] Nimit Sharad Sohoni, Christopher Richard Aberger, Megan Leszczynski, Jian Zhang, and Christopher Ré. Low-memory neural network training: A technical report. *arXiv preprint arXiv:1904.10631*, 2019.
- [50] Liuyihan Song, Pan Pan, Kang Zhao, Hao Yang, Yiming Chen, Yingya Zhang, Yinghui Xu, and Rong Jin. Large-scale training system for 100-million classification at alibaba. In *Proceedings of the 26th ACM SIGKDD International Conference on Knowledge Discovery & Data Mining*, pages 2909–2930, 2020.
- [51] Jakub M Tarnawski, Amar Phanishayee, Nikhil Devanur, Divya Mahajan, and Fanny Nina Paravecino. Efficient algorithms for device placement of dnn graph operators. *Advances in Neural Information Processing Systems*, 33:15451–15463, 2020.
- [52] Rajeev Thakur, Rolf Rabenseifner, and William Gropp. Optimization of collective communication operations in mpich. *The International Journal of High Performance Computing Applications*, 19(1):49–66, 2005.
- [53] John Thorpe, Yifan Qiao, Jonathan Eyolfson, Shen Teng, Guanzhou Hu, Zhihao Jia, Jinliang Wei, Keval Vora, Ravi Netravali, Miryung Kim, et al. Dorylus: Affordable, scalable, and accurate GNN training with distributed CPU servers and serverless threads. In *15th USENIX Symposium on Operating Systems Design and Implementation (OSDI 21)*, pages 495–514, 2021.
- [54] Parichehr Vahidinia, Bahar Farahani, and Fereidoon Shams Aliee. Cold start in serverless computing: Current trends and mitigation strategies. In *2020 International Conference on Omni-layer Intelligent Systems (COINS)*, pages 1–7. IEEE, 2020.
- [55] Ao Wang, Jingyuan Zhang, Xiaolong Ma, Ali Anwar, Lukas Rupperecht, Dimitrios Skourtis, Vasily Tarasov, Feng Yan, and Yue Cheng. InfiniCache: Exploiting Ephemeral Serverless Functions to Build a Cost-Effective Memory Cache. In *18th USENIX Conference on File and Storage Technologies (FAST 20)*, pages 267–281. usenix.org, 2020.
- [56] Hao Wang, Di Niu, and Baochun Li. Distributed machine learning with a serverless architecture. In *IEEE INFOCOM 2019-IEEE Conference on Computer Communications*, pages 1288–1296. IEEE, 2019.
- [57] Liang Wang, Mengyuan Li, Yinqian Zhang, Thomas Ristenpart, and Michael Swift. Peeking behind the curtains of serverless platforms. In *2018 USENIX Annual Technical Conference (USENIX ATC 18)*, pages 133–146, 2018.
- [58] Linnan Wang, Rodrigo Fonseca, and Yuandong Tian. Learning search space partition for black-box optimization using monte carlo tree search. In *Advances in Neural Information Processing Systems (NeurIPS)*, 2020, December 2020.
- [59] Ingo Wawrzoniak, Mike and Fraga Barcelos Paulus Bruno. Boxer: Data analytics on network-enabled serverless platforms. In *11th Annual Conference on Innovative Data Systems Research*, 2021.
- [60] Fei Xu, Yiling Qin, Li Chen, Zhi Zhou, and Fangming Liu. λ dnn: Achieving predictable distributed dnn training with serverless architectures. *IEEE Transactions on Computers*, 71(2):450–463, 2021.
- [61] Minchen Yu, Zhifeng Jiang, et al. Gillis: Serving large neural networks in serverless functions with automatic model partitioning. In *2021 IEEE 41st International Conference on Distributed Computing Systems (ICDCS)*, pages 138–148. IEEE, 2021.

- [62] Tian Zhang, Dong Xie, Feifei Li, and Ryan Stutsman. Narrowing the gap between serverless and its state with storage functions. In *Proceedings of the ACM Symposium on Cloud Computing*, pages 1–12, 2019.
- [63] Wei Zhang, Suyog Gupta, Xiangru Lian, and Ji Liu. Staleness-aware async-sgd for distributed deep learning. *arXiv preprint arXiv:1511.05950*, 2015.
- [64] Zhen Zhang, Chaokun Chang, Haibin Lin, Yida Wang, Raman Arora, and Xin Jin. Is network the bottleneck of distributed training? In *Proceedings of the Workshop on Network Meets AI & ML*, pages 8–13, 2020.
- [65] Yiyang Zhao, Linnan Wang, Kevin Yang, Tianjun Zhang, Tian Guo, and Yuandong Tian. Multi-objective optimization by learning space partitions. *10th International Conference on Learning Representations, ICLR*, 2022.

A Notations

The notations for Section 3.4 is summarized in Table 2.

B Iteration Time

Forward time. The forward time t_f is

$$t_f = t_f^0 + (\mu - 1)\Delta_f,$$

where t_f^0 is the time for the first micro-batch to traverse the forward pipeline, Δ_f the lag between consecutive micro-batches at the end of the forward pipeline, and μ the number of micro-batches per worker. The time t_f^0 is given by

$$t_f^0 = \sum_{i=1}^L t_{fc}^i + \sum_{i=1}^{L-1} (t_{fu}^i + t_{fd}^i),$$

where t_{fc}^i is the forward computation time of layer i , t_{fu}^i the upload time of the output of layer i to the storage, and t_{fd}^i the download time of the output of layer i from the storage to layer $i+1$. The individual terms are related to $(z_{i,j})$ by

$$\begin{aligned} t_{fc}^i &= \beta \sum_{j=1}^J z_{i,j} T_{fc}^{i,j}, & 1 \leq i \leq L, \\ t_{fu}^i &= x_i \left(\sum_{j=1}^J z_{i,j} \frac{o_i}{W_j} + t_{lat} \right), & 1 \leq i \leq L-1, \\ t_{fd}^i &= x_i \left(\sum_{j=1}^J z_{(i+1),j} \frac{o_i}{W_j} + t_{lat} \right), & 1 \leq i \leq L-1, \end{aligned} \quad (8)$$

where $T_{fc}^{i,j}$ is the forward computation time of layer i by a worker with memory M_j , $\beta \geq 1$ is the average slowdown factor due to resource contention when we overlap computation and communication, o_i is the output size of layer i , W_j is the bandwidth of a worker with memory M_j , and t_{lat} is the measured latency to storage. The values of $T_{fc}^{i,j}$, β , W_j and t_{lat} are measured by the *Model Profiler* during initial profiling. Note that communication times t_{fu}^i and t_{fd}^i are nonzero only if $x_i = 1$, i.e. there is a partition boundary after layer i .

The lag Δ_f is the maximum time of all stages, i.e.

$$\Delta_f = \max \left\{ \hat{t}_{fc}^{1:L}, t_{fu}^{1:(L-1)}, t_{fd}^{1:(L-1)} \right\}, \quad (9)$$

where $t^{i_1:i_2}$ denotes the set of variables t^i for $i_1 \leq i \leq i_2$, and \hat{t}_{fc}^i is related to t_{fc}^i by (4). For $i \in \mathcal{L}$, t_{fc}^i is the computation time for the stage containing layer i . For the example in Fig. 3, \hat{t}_{fc}^3 is the time for the second computation stage, consisting of layer 2 and layer 3. Note we only need to include \hat{t}_{fc}^i for $i \in \mathcal{H}$, but the inclusion of the other i gets rid of \mathcal{H} .

Backward time. The backward pipeline is similar. The backward computation time t_{bc}^i of layer i , the upload and download time t_{bu}^i, t_{bd}^i between layers i and $i-1$ are given by

$$\begin{aligned} t_{bc}^i &= \beta \sum_{j=1}^J z_{i,j} T_{bc}^{i,j}, & 1 \leq i \leq L, \\ t_{bu}^i &= x_{i-1} \left(\sum_{j=1}^J z_{i,j} \frac{g_i}{W_j} + t_{lat} \right), & 2 \leq i \leq L, \\ t_{bd}^i &= x_{i-1} \left(\sum_{j=1}^J z_{(i-1),j} \frac{g_i}{W_j} + t_{lat} \right), & 2 \leq i \leq L, \end{aligned}$$

where g_i is the gradient size from layer i to layer $i-1$. The cumulative backward computation time \hat{t}_{bc}^i from the previous partition boundary down to layer i is given by

$$\hat{t}_{bc}^L = t_{bc}^L, \quad \hat{t}_{bc}^i = t_{bc}^i + \hat{t}_{bc}^{i+1}(1 - x_i), \quad 1 \leq i \leq L-1. \quad (10)$$

For each $1 \leq i \leq L$, define

$$t_b^i = \sum_{k=i}^L t_{bc}^k + \sum_{k=i+1}^L (t_{bu}^k + t_{bd}^k) + (\mu - 1)\Delta_b^i, \quad (11)$$

where

$$\Delta_b^i = \max \left\{ \hat{t}_{bc}^{i:L}, t_{bu}^{(i+1):L}, t_{bd}^{(i+1):L} \right\}.$$

When i is the lowest layer of a partition, t_b^i is the computation completion time of that partition, and Δ_b^i is the corresponding lag between consecutive micro-batches. Note that $t_b^i \geq t_b^{i'}$ if $i' \geq i$ and layers i and i' belong to the same partition.

Synchronization time. For $i \in \mathcal{L}$, the synchronization time of the partition containing layer i is

$$t_s^i = (1 - y_1) \left(\sum_{j=1}^J z_{ij} \frac{\hat{s}_i}{W_j} \cdot \gamma + t_{lat} \cdot \delta \right), \quad (12)$$

where γ and δ are parameters that depend on the design of the synchronization method. For the *pipelined scatter-reduce*, we have $\gamma = 2$ and $\delta = 2 + d$ by (2). The model update time is negligible and hence not included. Note t_s^i is positive only if the degree of data parallelism is more than 1, i.e. $y_1 \neq 1$. We can use (12) to define t_s^i for other layers. Note that $t_s^i \geq t_s^{i'}$ if $i' \geq i$ and layers i and i' belong to the same partition.

C Linearization

First we present the major linearization techniques used to convert the non-linear binary integer programming to MIP:

Technique 1: Linearizing the multiplication of two binary variables. $x, y \in \{0, 1\}$, xy can be linearized as follows:

Notation	Definition
s_0	basic memory consumption of a serverless worker
M	total number of micro-batches
L	number of model layers.
P	unit price of serverless function
t_{lat}	latency from serverless worker to cloud storage
s_i	model size of layer i
a_i	size of activations of layer i per micro-batch
o_i	size of output of layer i per micro-batch
g_i	size of gradients from layer i to layer $i - 1$ per micro-batch
β	slowdown factor for computation due to resource contention
K	number of data parallelism options
D_k	value of k -th data parallelism option
J	number of resource allocation options
M_j	memory size of j -th resource option
W_j	bandwidth of j -th resource option
$T_{fc}^{i,j}$	forward computation time of layer i with j -th resource option
$T_{bc}^{i,j}$	backward computation time of layer i with j -th resource option
x_i	$\{0, 1\}$, 1 means model is partitioned between layers i and $i + 1$
y_k	$\{0, 1\}$, 1 means the k -th data parallelism option D_k is chosen
$z_{i,j}$	$\{0, 1\}$, 1 means layer i workers have j -th memory size M_j
t_{iter}	iteration time
c_{iter}	iteration cost
t_f	forward time for full forward pipeline
t_f^0	time for one micro-batch traverse forward pipeline
Δ_f	lag between micro-batches at end of forward pipeline
t_b^i	backward time until layer i completes computation
t_s^i	model synchronizing time at layer i
t_{fu}^i	time for layer i to upload its output to storage.
t_{fd}^i	time for layer $i + 1$ to download input from storage.
t_{bu}^i	time for i to upload gradient output to storage.
t_{bd}^i	time for layer $i - 1$ to be download gradient from storage.
d	degree of data parallelism, $d = \sum_{k=1}^K y_k D_k$
μ	number of micro-batches per worker, $\mu = M/d$
m_i	memory size of layer i worker, $m_i = \sum_{j=1}^J z_{i,j} M_j$
w_i	bandwidth of layer i worker, $w_i = \sum_{j=1}^J z_{i,j} W_j$
\hat{a}_i	accumulated activation size at layer i .
\hat{s}_i	accumulated model size at layer i .
\hat{t}_{fc}^i	accumulated forward computation time at layer i .
\hat{t}_{bc}^i	accumulated backward computation time at layer i .

Table 2: Notations

$$\begin{aligned}
f &= xy \\
f &\leq x \\
f &\leq y \\
f &\geq x + y - 1 \\
f &\in \{0, 1\}
\end{aligned} \tag{13}$$

Technique 2: Linearizing the multiplication of a continuous variable and a binary variable. $x \in \{0, 1\}$, $y \in [a, b]$ is a continuous variable, xy can be linearized as follows:

$$\begin{aligned}
f &= xy \\
f &\leq y \\
f &\geq y - b(1 - x) \\
ax &\leq y \leq bx
\end{aligned} \tag{14}$$

Technique 3: Linearizing of the max operator. x, y, z are continuous variables, $\max\{x, y, z\}$ can be linearized as follows:

$$\begin{aligned}
f &= \max\{x, y, z\} \\
x &\leq f, y \leq f, z \leq f \\
x &\geq f - H(1 - l_1) \\
y &\geq f - H(1 - l_2) \\
z &\geq f - H(1 - l_3) \\
l_1 + l_2 + l_3 &\geq 1 \\
l_1, l_2, l_3 &\in \{0, 1\}
\end{aligned} \tag{15}$$

where H is a large constant. Next we introduce how we linearize the formulation in detail.

1. *Linearizing the equality constraint for the cumulative values \hat{t}_{fc}^i , \hat{t}_{bc}^i , \hat{s}_i and \hat{a}_i .* We introduce \hat{t}_{fc}^i , \hat{t}_{bc}^i , \hat{s}_i and \hat{a}_i as continuous variables and linearize their equality constraints. We use \hat{t}_{bc}^i in (10) as an example and it is similar with the others. We can write \hat{t}_{bc}^i as:

$$\begin{aligned}
r_i &= 1 - x_i \\
\hat{t}_{bc}^i &= t_{bc}^i + \hat{t}_{bc}^{i+1} r_i \\
&= \sum_{q=i}^L t_{bc}^q \prod_{p=i}^{q-1} r_p
\end{aligned} \tag{16}$$

Since r_i is a binary variable, $\prod_{p=i}^{q-1} r_p$ can be converted to a new binary variable $\hat{r}_{i,q}$ by recursively performing linearization with **Technique 1**. Then continuous variable \hat{t}_{bc}^i satisfies the following constraint

$$\begin{aligned}
\hat{t}_{bc}^i &= \sum_{q=i}^L t_{bc}^q \hat{r}_{i,q} \\
&= \beta \sum_{q=i}^L \sum_{j=1}^J z_{i,j} \hat{r}_{i,q} T_{bc}^{i,j}
\end{aligned} \tag{17}$$

$z_{i,j}$ and $\hat{r}_{i,q}$ are both binary variables, thus $z_{i,j} \hat{r}_{i,q}$ can be linearized applying **Technique 1**.

2. *Linearizing the equality constraint for t_{fu}^i , t_{fd}^i , t_{bu}^i and t_{bd}^i .* We introduce t_{fu}^i , t_{fd}^i , t_{bu}^i and t_{bd}^i as continuous variables and linearize their equality constraints. We use t_{fu}^i as an example and it is similar with the others. We can write t_{fu}^i in (8) as:

$$t_{fu}^i = \sum_{j=1}^J x_i z_{i,j} \frac{o_i}{W_j} + x_i t_{lat} \tag{18}$$

x_i and $z_{i,k}$ are both binary variables, thus $x_i z_{i,j}$ can be linearized applying **Technique 1**.

3. *Linearizing forward time t_f and backward time t_b^i .* We use t_b^i as an example and it is similar with t_f . Linearizing t_b^i in (11) is equal to linearizing $(\mu - 1)\Delta_b^i$. Since Δ_b^i is the max of a set of continuous variables, it can be presented as a continuous variable with linear constraints using **Technique 3**. Expand $(\mu - 1)\Delta_b^i$, we have

$$(\mu - 1)\Delta_b^i = \sum_{k=1}^K \Delta_b^i y_k \frac{M}{D_k} - \Delta_b^i \tag{19}$$

Since Δ_b^i is a continuous variable and y_k is a binary variable, $\Delta_b^i y_k$ can be linearized applying **Technique 2**.

4. *Linearizing t_s^i .* Expand (12), we have

$$t_s^i = \sum_{j=1}^J (z_{ij} \hat{s}_i - y_1 z_{ij} \hat{s}_i) \frac{\gamma}{W_j} + (1 - y_1) t_{lat} \cdot \delta, \tag{20}$$

z_{ij} and y_1 are binary variables, \hat{s}_i is a continuous variable, thus we can first linearize $z_{ij} \hat{s}_i$ using **Technique 2** and then further linearize $y_1 z_{ij} \hat{s}_i$ by applying **Technique 2** again.

5. *Linearizing full iteration time t_{iter} .* So far we have linearized t_f , t_b^i and t_s^i in (7). We can further remove the max operator using **Technique 3**.

6. *Linearizing total memory allocation c_{mem} .* Expand (5), we have

$$c_{mem} = \sum_{i=1}^{L-1} \sum_{k=1}^K \sum_{j=1}^J x_i y_k z_{i,j} D_k M_j + \sum_{k=1}^K \sum_{j=1}^J y_k z_{L,j} D_k M_j \tag{21}$$

Since x_i , y_k , and $z_{i,j}$ are all binary variables, $x_i y_k z_{i,j}$ and $y_k z_{L,j}$ can be linearized using **Technique 1**.

7. *Linearizing memory constraint.* At last, we linearize the memory constraint, the first constraint in (3). Expand the constraint, we have

$$\sum_{k=1}^K \hat{a}_i y_k \frac{M}{D_k} + 4\hat{s}_i - 2\hat{s}_i y_1 + s_0 \leq \sum_{j=1}^J z_{i,j} M_j \tag{22}$$

$\hat{a}_i y_k$ and $\hat{s}_i y_1$ can both be linearized with **Technique 2**.

After linearization, t_{iter} , c_{mem} and the constraints in (3) are all in linear form. c_{iter} ((6)) and the objective function are quadratic. The formulation becomes a mixed-integer quadratic program. It has a total of $\max\{o(JL^2), o(JKL)\}$ integer variables, $\max\{o(JL), o(KL)\}$ continuous variables and $\max\{o(JL^2), o(JKL)\}$ linear constraints.

Model	Batchsize			Average
	16	64	256	
<i>ResNet101</i>	5.9%	11.2%	15.4%	10.8%
<i>Amoebanet-D18</i>	13.3%	9.0%	10.6%	11.0%
<i>Amoebanet-D36</i>	10.8%	4.0%	18.1%	11.0%
<i>Bert-large</i>	9.8%	11.0%	16.4%	12.4%
Average	9.9%	8.8%	15.1%	11.3%

Table 3: **Prediction error of training tasks.** Our performance model achieves an average prediction error of less than 12%.

D Details of Baseline Methods

The serverless-based training designs used in the evaluation and their resource allocation strategies are summarized as follows:

- **LambdaML** follows a pure serverless-based training design. It uses the maximum memory allocation and maximum local batch size within the memory limit for each worker. This strategy reduces the number of workers used for training for a given global batch size.
- **HybridPS** follows a hybrid PS training design and requires the use of parameter servers. We select the instance with the lowest cost that can perform our tasks without incurring CPU or memory bottleneck as the parameter server, i.e. a *c5.9xlarge* instance on AWS, and a *r7.2xlarge* instance on Alibaba. The resource allocation of workers follows the same strategy as that of LambdaML. Note that we replace the data serialization API in the implementation with the python `pickle` module to better utilize the worker network bandwidth. Prior to this modification, the implementation can only achieve a throughput of about 20MB/s; the current implementation can fully utilize the bandwidth at about 70MB/s. We test this modification on the models and observe improvement in both training speed and cost.
- **LambdaML-GA** applies gradient accumulation to the LambdaML baseline. It uses the same number of workers as LambdaML but allocates *the minimum memory* required after performing gradient accumulation for each worker.
- **HybridPS-GA**. HybridPS with gradient accumulation. It follows the similar resource allocation strategy as that of LambdaML-GA.

The details of the baseline partition and resource allocation algorithms used in the evaluation, i.e. TPDMP and Bayes are as follows

- **TPDMP** is the latest graph-based model partition algorithm for server-based pipeline training [51]. It focuses on maximizing the pipeline training throughput with a fixed amount of resource. To apply the algorithm to the serverless scenario, we perform a grid search on the resource allocation and optimizes the model partition with *TPDMP* for each allocation. We select the configuration that minimizes the objective function in (3).
- **Bayes** is a blackbox optimization method that has been proved effective in deciding configurations for cloud services [4]. It generates a configuration, measures its performance, and iteratively refines the decision. It can be used to jointly optimize the model partition and resource allocation. However, with the search space of this problem, *Bayes* can require many iterations just to find a feasible configuration. For example, it fails to find a feasible configuration for over half of our training tasks with 20 iterations. To reduce the prohibitive time cost of real-world measurement, we evaluate each configuration with our performance model that has a high accuracy of 88% as shown in Appendix E. Using performance models in place of the actual measurement is recently proposed and demonstrated to produce good optimization performance [58, 65]. We run a total of 100 iterations to minimize the objective function.

E Performance Model Accuracy

Table 3 displays the prediction error in training time for the measured points of FUNCPipe in Fig. 6. The results show that our performance model achieves an average prediction error of less than 12%. The largest error happens when training *Amoebanet-D36* with a global batch size of 256. We note that this error is mainly caused by the unexpected bandwidth variation; other model training is less impacted as they use fewer serverless workers and are less subject to the performance interference among workers. We leave the consideration of such interference in our performance model as part of future work.